Control of Temperature Nonuniformity Based on Line-of-Sight Absorption

Tudor I. Palaghita[*] and Jerry M. Seitzman[†]
Georgia Institute of Technology,
Daniel Guggenheim School of Aerospace Engineering,
Atlanta, GA, 30332

This paper describes the development and demonstration of a sensing approach for control of temperature nonuniformity (pattern factor) based on diode laser line-of-sight water absorption near 2 μm. A temperature nonuniformity variable is defined based on the difference in temperatures measured with two pairs of water lines. To reduce the complexity of the system the sensor relies on the ratio of the absorption line peaks rather than the more common, integrated absorption. Selection of appropriate lines and factors influencing sensor performance are described. Open loop control with this sensor is demonstrated in the exhaust plane of a stratified methane-air combustor. The exit temperature profile can be altered by changing the flow rates to two upstream injectors or with a synthetic jet mixing actuator. In both cases, the nonuniformity variable tracks the mixidness of the flow.

I.   Introduction

New gas turbine engine designs are driven by the need for increased engine efficiencies, reduced environmental impact, and improved maintainability. This is true for both ground-based and aero-engines. To reach the desired levels of fuel economy, emissions and lifetime, control systems will likely have to be employed at all levels of operation. These intelligent engine systems can help reduce emissions, ensure safer operation and enable real-time engine system health monitoring. Sensing and control strategies are especially important at off-design operating conditions and as the engines ages. Pattern factor sensing and control is one element of the intelligent engine concept. For example, pattern factor (temperature profile) control can be used to increase turbine-blade lifetime. It may also help decrease combustor emissions through control of mixing in the combustor, and can be used for health monitoring.

Development of sensors is a key step required for effective control systems. Optical sensing techniques are a natural choice for combustion environments because they are non-intrusive, fast, and can be used in the extreme conditions associated with combustion. Diode laser based, active sensing approaches offer many advantages. Because of their commercial applications in telecommunications, diode lasers are relatively cheap and widely available, making them ideal light-sources for optical combustion sensors. Other advantages of diode lasers are their compatibility with fiber optics, fast response time, narrow spectral features, and good sensitivity. They are also small, rugged, and tunable

Diode laser absorption-based combustion sensors for temperature, pressure, velocity, and species concentrations have been demonstrated both in the laboratory and in limited *in situ* applications.[1-4] Generally these sensors use the easy tuning ability of diode lasers to resolve spectral features and compute path-averaged quantities of interest in combustion flows.

In this paper, we describe and demonstrate an optical sensing approach for temperature nonuniformity based on line-of-sight water absorption near 2 μm. Our goal is to develop a sensor for pattern-factor control that is fast and relatively simple to implement in gas-turbine engines. Water was chosen as the marker species because it is a major combustion product that has relatively strong absorption lines throughout a large portion of the spectrum (Fig. 1). Moreover, it is easy to find water lines with little or no interference from other combustion products. It is important to note that the sensor is not intended to provide especially accurate temperature measurements, but rather is designed for sensing changes in the temperature profile with good time response. The rotational-vibrational

---

[*]Graduate Research Assistant, School of Aerospace Engineering, AIAA Student member
[†]Associate Professor, School of Aerospace Engineering, AIAA Associate Fellow

American Institute of Aeronautics and Astronautics

transitions used in this paper (between 1950 and 2030nm) were chosen based on the available laser hardware. The same methodology can be used at other wavelengths and with other species based on available lasers.

II. Absorption Theory

The narrowband absorption of a light signal at wavelength ν (cm^{-1}) with incident intensity I_0 and transmitted intensity $\underline{I}$ by a medium of thickness L (cm), is described by the Beer-Lambert Law:

$$\frac{I}{I_0}(\nu) = e^{\int_0^L - pxS_i(T)\phi(\nu-\nu_0,T,x,p)dl} \tag{1}$$

Figure 1. Representative absorption spectrum for 10% water in air (data from HITEMP).

where p is the pressure (atm), x is the absorber mole fraction, S is the line strength (cm^{-2} atm^{-1}) of the ith transition (centered at ν_0), T is the temperature (K), and ϕ is the line shape function whose integral is normalized to unity. For a particular transition i centered at $\nu_{0,i}$, the line strength S is a function of temperature only:

$$S_i(T) \approx S_i(T_0)\frac{Q(T_0)}{Q(T)}\frac{T_0}{T}\exp\left(-\frac{hcE''}{k}\left(\frac{1}{T}-\frac{1}{T_0}\right)\right) \cdot \left[1-\exp\left(\frac{-hc\nu_{0,i}}{kT}\right)\right] \cdot \left[1-\exp\left(\frac{-hc\nu_{0,i}}{kT_0}\right)\right]^{-1} \tag{2}$$

where Q is the partition function, E'' is the lower state energy of the transition (cm^{-1}), h is Plank's constant, c is the speed of light, and k is Boltzmann's constant. T_0 is a reference temperature, taken here to be 296K, consistent with the HITEMP[5] database. The last two terms account for the effect of stimulated emission and can generally be neglected at wavelengths below 2.5 μm and temperatures below 2500 K.

In a medium with uniform properties (temperature and concentration), one can determine the temperature and mole fraction of the species of interest by probing two absorption lines. By integrating over a frequency band centered at ν_0, the line shape function is eliminated and the ratio of the absorptivity of two lines becomes a function of temperature only:

$$abs_i = \int_{-\infty}^{\infty} -\ln\left(\frac{I}{I_0}(\nu)\right)d\nu = \int_{-\infty}^{\infty}\int_0^L p \cdot x \cdot S_i(T)\phi_i(\nu-\nu_0,T,x,p)dld\nu = pxS_i(T)L \tag{3}$$

$$R_{ij} = \frac{abs_i}{abs_j} = \frac{S_i(T)}{S_j(T)} = \frac{S_i(T_0)}{S_j(T_0)}\exp\left(-\frac{hc}{k}(E_i''-E_j'')\left(\frac{1}{T}-\frac{1}{T_0}\right)\right) \tag{4}$$

Using the absorbance of two lines one can determine the temperature of the gas using Eq. (4) and the concentration of the species of interest using Eq. (3). In this gas with uniform properties, any two lines we pick would yield the same results (neglecting experimental errors).

A. Nonuniform flow properties

When the temperature and concentration of the medium are not uniform, as is the case in a combustor, the integral in Eq. (3) cannot be solved without prior knowledge of the temperature (and concentration) profile. For an arbitrary temperature and concentration profile along the line of sight, the ratio of the absorbances of 2 lines i and j becomes:
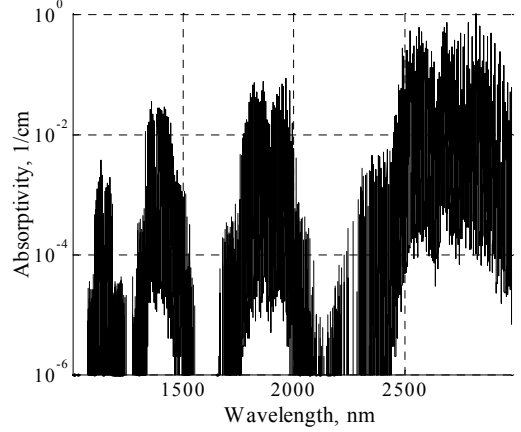
$$R_{ij} = \frac{abs_i}{abs_j} = \frac{\int_0^L xS_i(T)dl}{\int_0^L xS_j(T)dl} \tag{5}$$

This ratio can be written as:

$$R_{ij} = \frac{abs_i}{abs_j} = \frac{S_i(T_{ij})}{S_j(T_{ij})} \tag{6}$$

where T_{ij} is the "average" temperature that would be found by assuming uniform properties across the path. Because S is a nonlinear function of T, the integrals in Eq. (5) represent a nonlinear averaging process. This means that the ratio of the absorbances becomes a function of the two chosen lines. The average temperature T_{ij} will depend on the chosen line pair because each line has a different dependence on temperature. This result will also depend in great measure on the correlation between concentration and temperature. The more we know about how the mole fraction and temperature are related, the more meaningful T_{ij} becomes.

While no discrete spatial information can be obtained when using only one line of sight sensor, one can compute various "average" temperatures by measuring several pairs of lines. These different temperatures can yield information about the degree of temperature uniformity of the flow. As the temperature profile becomes uniform, these temperatures (T_{ij}) will converge to the same number. This fact can be used to measure the degree of nonuniformity in the flow. Previous work at Georgia Tech[6,7] used numerical simulation of water absorption using the HITEMP database. It was shown that with three appropriately chosen absorption lines one can monitor for the presence of hot or cold spikes in the exhaust flow of a high-pressure combustor. A similar approach was later applied to measurements of O_2 profiles in static heated cells of air.[8] Many closely spaced absorption lines were measured and used to compute the mole fraction or column-density of O_2 corresponding to predefined temperature bins expected in the gas.

B. Peak absorption ratios

The vast majority of previous work on diode laser sensors in combustion used integrated absorbances (Eq. (4)) for determining temperature. An alternate approach is the use of the maximum absorption at the line peak, a, instead of the absorbances:

$$a = -\ln\left(\frac{I}{I_0}(\nu_0)\right) = \int_0^L p \cdot x \cdot S(T)\phi(\nu = \nu_0, T, x, p)dl \tag{7}$$

The ratio of the absorption for the peaks of two lines is then:

$$A_{ij} = \frac{a_i}{a_j} = \frac{\int_0^L x \cdot S_i(T)\phi_i(\nu = \nu_{0i}, T, x, p)dx}{\int_0^L x \cdot S_j(T)\phi_j(\nu = \nu_{0j}, T, x, p)dx} \xrightarrow{\text{uniform x}} \frac{S_i(T_{ij})\phi_i(\nu_{0i}, T_{ij})}{S_j(T_{ij})\phi_j(\nu_{0j}, T_{ij})} \tag{8}$$

The use of integrated absorbances results in more accurate temperature measurements in mediums with uniform properties because the line-shape function, ϕ, depends on broadening parameters that are usually not very well known and on the path-dependent properties (T, x). However, measuring absorbances requires lasers with good tuning characteristics, a way to accurately measure wavelength, and more demanding computational capabilities as well as longer computational times. The alternative is to measure the peak absorption and use it to determine temperature (Eq. (8)). This method reduces computational time, hardware complexity, and the time response of the sensor. When using a single tuning laser to measure several absorption peaks, it is straightforward to identify the peak wavelength, eliminating the need for an etalon or wavemeter to monitor laser wavelength during tuning. Alternately, multiple (fixed wavelength) lasers can be used to monitor several line-peaks.

Another advantage of using peak absorptions is that a sensor based on line-peaks instead of absorbances will also work well at high pressures where lines broaden significantly and individual features are very difficult to

distinguish.[9] Also, in many cases, the ratio of peak absorptions can be approximated by the ratio of absorbances, or, if the lines are chosen to be rather insensitive to pressure and to have similar broadening characteristics, a simple correction can be used to yield results comparable to using integrated absorbances.[8,3] For these reasons, the current approach employs peak ratio measurements to track the degree of temperature nonuniformity or mixedness of the gas.

C. Broadening effects

In the peak ratio approach, one must consider line broadening characteristics when selecting appropriate absorption lines for the sensor. Broadening comes into play through the ratio of line shape functions in Eq. (8). At combustion temperatures, both Doppler and pressure broadening are important. The line shape function (ϕ) can be represented by a Voigt profile, the convolution of Lorentzian collision broadening and Gaussian Doppler broadening, as given by:

$$\phi(D,B) = \frac{1}{\Delta\nu_D}\sqrt{\frac{\ln 2}{\pi}}K(D,B) = \frac{1}{\Delta\nu_D}\sqrt{\frac{\ln 2}{\pi}}\frac{B}{\pi}\int_{-\infty}^{\infty}\frac{e^{-y^2}}{B^2+(D-y)^2}\,dy \tag{9}$$

$$D = \sqrt{\ln 2}\,\frac{\nu-\nu_0}{\Delta\nu_D} \qquad \text{and} \qquad B = \sqrt{\ln 2}\,\frac{\Delta\nu_c}{\Delta\nu_D} \tag{10}$$

where $\Delta\nu_D$ and $\Delta\nu_c$ are the Doppler and collision broadening widths. The Doppler width of a line is a function of the root of the temperature (c_1 is a constant for a given molecule):

$$\Delta\nu_D = c_1\nu_0\sqrt{T} \tag{11}$$

Collision broadening of an absorbing molecule depends on gas composition, as each collision partner has different broadening parameter γ_k and temperature coefficient n_k. This dependence takes the general form of Eq. (12):

$$\Delta\nu_c = \sum_k \gamma_k \frac{P}{P_0}\left(\frac{T_0}{T}\right)^{n_k} x_k \tag{12}$$

At the line peak, $D = 0$, $\phi(0,B) = \phi(\nu=\nu_0,B)$, and peak absorption becomes a function of the broadening half-width ratio, B. We can now relate the absorbance ratio to the peak ratio of two lines:

$$R_{ij} \cong A_{ij}\frac{K(0,B_1)}{K(0,B_2)} = \frac{B_i\int_{-\infty}^{\infty}\frac{e^{-y^2}}{B_i^2+y^2}\,dy}{B_j\int_{-\infty}^{\infty}\frac{e^{-y^2}}{B_j^2+y^2}\,dy} \tag{13}$$

In a nonuniform flow, there are several factors that affect the K ratio in Eq. (13). First, uncertainties in the broadening characteristics of the lines (for example the temperature coefficient n, or the species broadening coefficients) will introduce uncertainties in the values of B. Another source of errors is the unknown concentration and composition distribution along the path. Variable water mole-fraction and unknown concentration of other species will change the value of B. Overall, if the temperature coefficient n is similar then the other unknowns have little effect on the B_i/B_j ratio that appears in Eq. (13). The largest effect comes from the integral part of K (Eqs. (9) and (13)). A sample line pair A/R ratio is plotted in Fig. 2. The two curves correspond to changes in broadening due to composition or other broadening uncertainties of about 25%. This figure shows that using the peak ratio (A) instead of integrated absorbance (R) will introduce errors. By selecting pairs of lines with similar broadening behavior, however, these errors can be kept small (~2%). Furthermore, broadening effects will have an even smaller effect on measuring changes in the temperature profile.

American Institute of Aeronautics and Astronautics

III. Sensor Operation

For a medium with nonuniform properties, the temperature from each separate line pair is computed from the following expression, where A_{ij} is the peak ratio:

$$T_{ij} = \left[\frac{1}{T_0} - \frac{1}{1.44(E_i - E_j)} \ln\left(A_{ij} \frac{S_{0j}}{S_{0i}} \right) \right]^{-1} \tag{14}$$

In the simplest case, three appropriately chosen absorption lines produce two independent temperatures, T_{12} and T_{13}. Based on these temperatures, we can define a nonuniformity variable:

$$U = \frac{|T_{12} - T_{13}|}{0.5 \cdot (T_{12} + T_{13})} = \frac{\Delta T}{\bar{T}} \tag{15}$$

This variable should approach zero when the gas is uniform, and increase as the temperature nonuniformity increases (or as the degree of mixing decreases). If more line pairs are measured, a new nonuniformity variable could be defined to take advantage of the additional information. Although having information from multiple lines can improve sensor performance, it also adds complexity to the system.
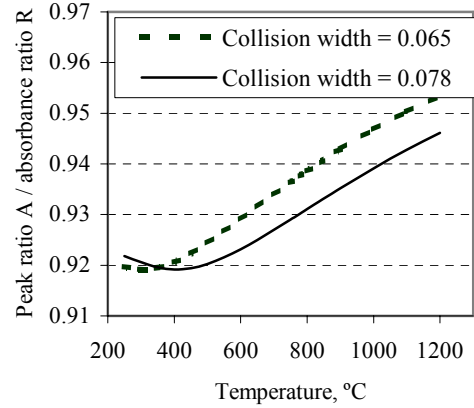
A. Line Selection

Selection of appropriate absorption lines has a great influence on sensor performance. Although line selection is specific to the expected sensor operating environment (e.g., temperature range) and hardware capabilities, a generic methodology for selecting appropriate absorption lines has been proposed.[3]

Absorption lines or transitions have different dependence on temperature, based on their spectroscopic properties. The reference line strength ratio in Eq. (14) determines the dynamic

Figure 2. Broadening effects on peak ratio.

range of the sensor, so lines with similar S_0 are desirable. From Eqs. (4) and (14), it is evident that the lower state energy difference ($\Delta E''$) of the transitions controls how the line changes with temperature. By differentiating Eq. (4) with respect to temperature, we can compute the sensitivity of the absorptivity ratio with respect to temperature:

$$\frac{\Delta R}{R} \bigg/ \frac{\Delta T}{T} = 1.44 \frac{\Delta E}{T} \tag{16}$$

A large $\Delta E''$ is desired for good sensitivity. Also, when selecting multiple line pairs, they should have different $\Delta E''$, such that the temperature dependence of the ratios is different. In a given temperature range, an absorption line can increase, decrease, or stay approximately constant with temperature. In the range of temperatures present in our combustor exhaust (100–1000 C) and based on the limitations of our laser and detector setup, we can only resolve lines with $S(T_0)$ above ~10^{-5} cm^{-2} atm^{-1} and with E'' in the range 100–3000 cm^{-1}. Generally, the lower E'' is for a line, the more its absorption is weighted towards lower temperatures (a "cold" line). Lines with high E'' require high temperatures before their lower state is populated, and thus their absorption is weighted towards hot gases ("hot" lines). Fig. 3 shows a plot of the calculated absorption spectrum at 200 ºC and 700 ºC for part of the wavelength range of our laser. It can be seen that some lines increase with temperature (hot lines a and b) while other lines decrease as the temperature increases (cold line c). For better temperature (and temperature uniformity) sensitivity, it is desirable to include hot and cold lines in the ratios.
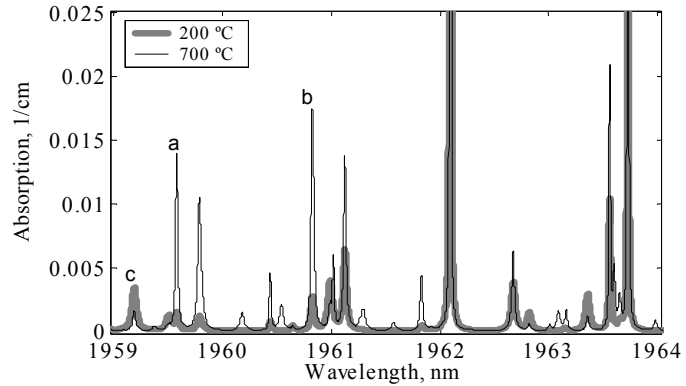
With the HITRAN spectroscopic database, we computed the peak absorption of several water lines as a function of temperature, for a gas with 10% water at 1 atm and uniform temperature and concentration (Fig. 4). As an example, lines 1, 2, and 4 in the figure are better suited than line 3. Lines 1 and 2 are sensitive to high temperatures, while line 4 is sensitive to lower temperatures. The ratios of line-peaks 1/2 and 2/4 are plotted in Fig. 5 and represent an example of desirable pairs: they have good but different sensitivity (slope) to temperature. By using the ratio of the hot line 1 to the intermediate line 2, we capture the effect of high temperatures, while the ratio of line 2 to 4 accentuates the cold regions. This choice of lines also gives similar ratio values, effectively normalizing the hottest and coldest lines.

Figure 3. Representative absorption spectrum for 20% water in air based on HITEMP data.
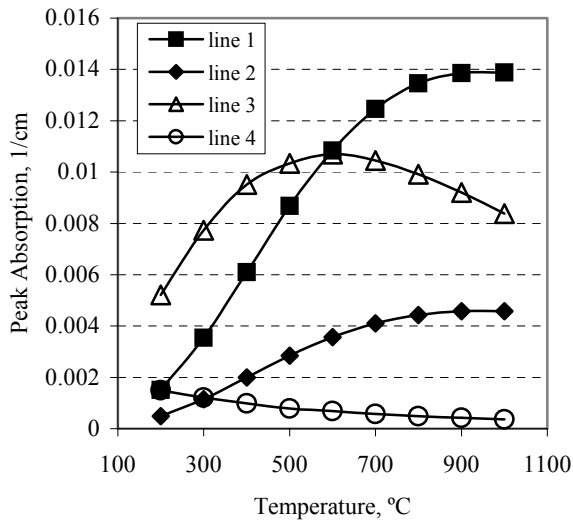
Another consideration in line selection is the broadening characteristics. As shown above, line pairs with similar broadening characteristics are desirable, as the broadening effects would cancel each other making changes in the peak ratios easier to interpret. Also, since broadening depends on composition, species effects could add a dependence on the unknown concentration distribution. On the other hand, differences in the temperature dependence of the collision broadening may in fact be beneficial if this dependence is such that temperature extremes are accentuated. Broadening variations due to composition changes, rather than temperature changes ((Eq. (13)) will limit the useful range of U, especially for near uniform temperature distributions, where uncertainties will effectively create a threshold below which changes in U will be meaningless.

IV. Experimental Setup

The experimental setup is presented in Fig. 6. The light source is a New Focus Velocity, external cavity tunable diode laser with a maximum power of 3.5 mW, operating between 1950–2040nm. The laser beam passes through a beam-splitter, with one beam sent to an InGaAs detector used to monitor the background room-air absorption. The second beam is double passed through the exhaust gases of a methane-air combustor with a second InGaAs detector used to measure the absorption of the beam at the combustor exhaust. The air-paths of the two detectors are matched. The voltage signal from the two detectors is captured by a computer data acquisition system.

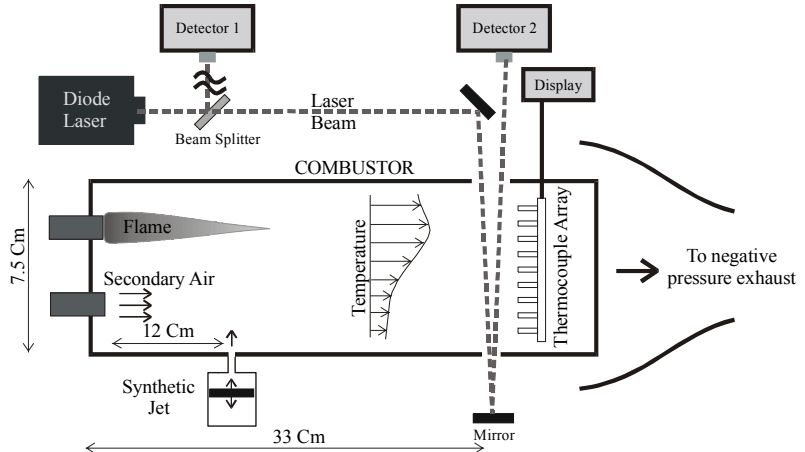

Figure 4. Temperature dependence of absorption line peaks.
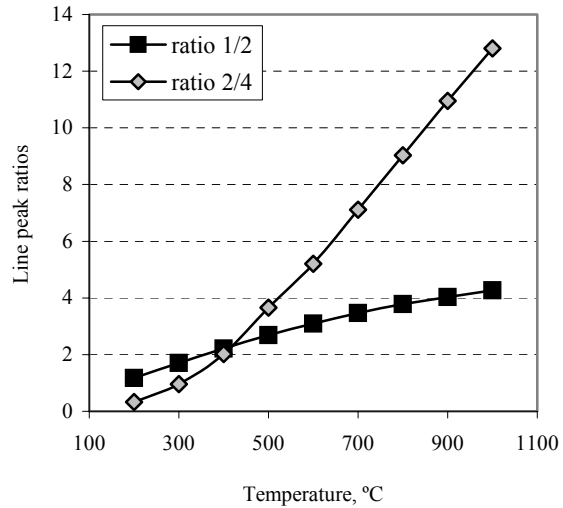
Figure 5.   Temperature dependence of ratios of absorption line peaks.

American Institute of Aeronautics and Astronautics

The combustor has a rectangular cross-section and two upstream injection systems. The primary fuel-air injector is located at the top of the combustor, and a secondary (dilution) air injector it is located at the bottom. The flow rates of methane, primary, and secondary air can all be varied independently. At the combustor exhaust, there is a vertical array of thermocouples just downstream of the laser path. Changes in the exhaust temperature profile can be obtained in two ways. First, the relative flow rates of the primary and secondary air can be changed. In this case, the total water content of the exhaust is kept constant if the total air supply rate remains the

Figure 6. Experimental Setup.

same. Another way to change the temperature profile is to enhance mixing between the cold air stream and the flame products. In the current setup, this is accomplished with an array of synthetic jets.[10,11]

A. Synthetic Jet

A synthetic jet is a mixing actuator that requires no external mass flow. It typically consists of a cavity with a small orifice leading to the flow of interest. The cavity volume is modulated such that it sucks fluid from the flow field during its expansion and ejects it in a jet like manner during its compression. In our implementation, the synthetic jet is a piston-cylinder system in the lower part of the combustion chamber. Therefore it can move cold fluid from the bottom of the stratified combustor into the hot region above and enhance the mixing. An electric motor is used to drive the piston and the fluid is ejected through an array of 4 small holes oriented perpendicular to the combustor flow. The mixing enhancement increases roughly with modulation frequency for our configuration, but at high frequencies the effects diminish.[10,11]

B. Laser system

The external cavity diode laser used here has two tuning modes: a slow tuning mode (up to 40nm/s which corresponds to a repetition rate of ~4Hz over several water lines) over the full tuning range of the laser; and a fast tuning mode (up to ~150Hz) over about 0.3nm. A sample slow scan is shown in Fig. 7. The large changes in laser power with wavelength are due to etalon effects in the laser cavity, and the small dips represent absorption lines. Measurement limitations arise because small changes in the absorption lines have to be measured over large changes in the incident laser power. Because of the difficulty in accurately fitting a background and because of unsteadiness in the combustor, the slow tuning mode of this laser is more difficult to use for sensor measurements. The large change in laser power is characteristic for external cavity lasers. More typical, commercially available lasers (though often with smaller tuning range) have much better tuning characteristics and would likely result in better sensor performance.

Thus, we present data acquired using fast tuning only with its limited wavelength range. This limits our measurements to one or two lines simultaneously. To obtain the two line pair ratios required to measure U, we rapid tune the laser many times (on the order of 1s) over one or two absorption lines, then slowly scan the laser to a new location and
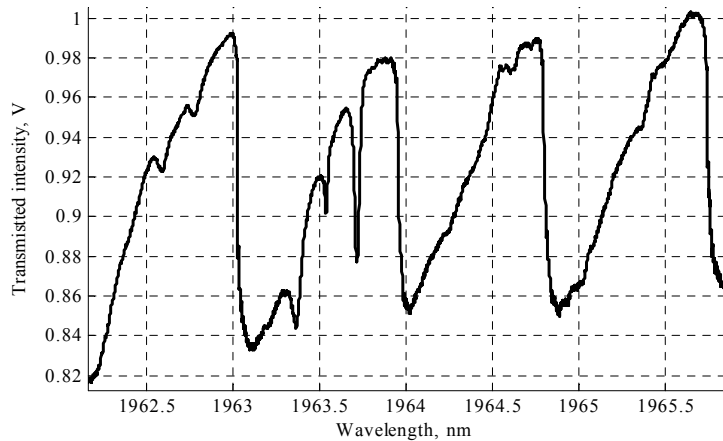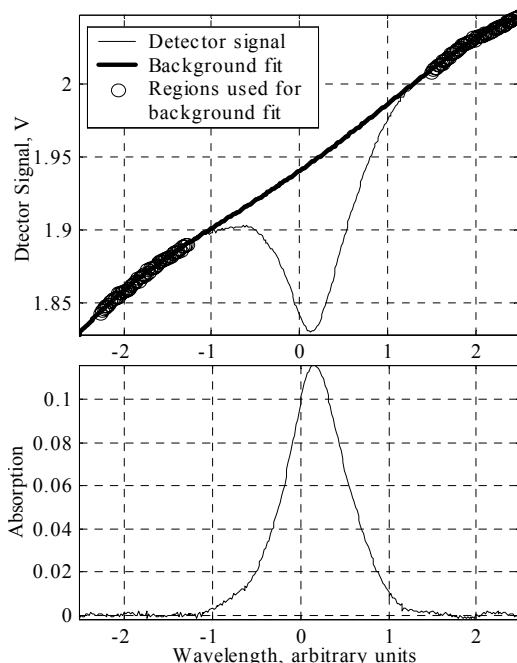

Figure 7. Slow laser tuning over a large wavelength range.

repeat the fast scans. Since not all the lines are captured at the same time, averages of multiple measurements are needed to decrease the effects of combustor unsteadiness and beam steering.

C. Signal Conditioning

The detector signals must be corrected to produce accurate absorption measurements. One must account for the changes in laser intensity due to scanning (noted above), beam walk and beam steering, and background absorption due to water in the room air. There are two methods to accomplish this. One can subtract balanced signals from the two detectors at each wavelength and then calculate the absorption at line center. This can be done quickly and does not require laser tuning, but does not correct for beam steering in the combustor or laser beam walk during cavity tuning. This method is also very sensitive to balancing errors between the detectors. In the second approach, one fits a background to each detector signal independently, using spectral regions with no water absorption (e.g., the far wings of an isolated absorption line). Because it is difficult to balance the detectors over the large range of intensities associated with the laser tuning, we employ this second method even though it is computationally more intensive.

The laser is fast tuned over an isolated line using a triangular driving wave at 80Hz. A half-period scan is shown at the top of Fig. 8. Regions far from the line center are used to fit

Figure 8. Half-period of fast laser scan over an isolated water absorption line. The top panel shows the detector trace and background fit, the bottom panel shows the resulting absorption, -ln(I/I₀).

a polynomial background on data from both detectors. We then compute the absorption, $-\ln(I/I_0)$, as seen at the bottom of Fig. 8, for data from both detectors and subtract room water absorption from the total absorption to determine the absorption in the combustor.

V. Results

Table 1 lists the water lines that were used in this work with their spectroscopic properties as given in the HITEMP database. The line-pairs used to determine the temperatures T_{ij} used in the computation of U are listed in Table 2. For a given set of combustor operating conditions, the average exhaust temperature profiles were obtained from the thermocouple data. These were then used to interpret the results of the laser sensor. Results are presented for the two mixing control methods described above: variations of the upstream air flow rates, and mixing control with the synthetic jet array.

A. Air injection control

In this approach, the total flow rates of methane and air were maintained at a constant value (4 scfh fuel, 152 scfh air), while the ratio of air supplied to the premixed burner (primary) and secondary air injector was varied. This

Line center 1/cm	Line center nm	$S(T_0)$ cm^{-1}/(molecule cm^{-2})	E" cm^{-1}	Air broadening γ_{air}	Self broadening γ_{self}	Temperature broadening coefficient, n	Line designation
5116.798	1954.347	3.61E-22	1201.922	0.0756	N/A	0.64	h1
5113.872	1955.465	2.5E-22	1293.634	0.0374	N/A	0.64	h2
5107.072	1958.069	1.14E-22	1446.129	0.0499	N/A	0.64	h3
5043.740	1982.656	3.18E-24	2246.888	0.0244	N/A	0.64	hh
5093.326	1963.354	2.02E-22	285.419	0.0830	N/A	0.64	c1
5105.400	1958.710	3.06E-23	704.214	0.0625	N/A	0.64	c3

Table 1.   Lines used for computing U and their spectroscopic properties from the HITEMP database.

changes the temperature of the upper (burning) stream, as well as the relative flow velocities of the two streams and the mixing characteristics between them. Two cases were examined, 54% of the air supplied to the premixed (primary) injector and 44%. The resulting temperature profiles for the two cases are shown in Fig. 9. As the flame is located in the top part of the combustor, the maximum temperatures can be seen in that region, with the peak at a nondimensional vertical location (normalized by the combustor height) of 0.7. In the first case (54% primary air), when there is a higher flow rate through the upper portion of the combustor (compared to the

Line pairs	S_{0i}/S_{0j}	ΔE, cm^{-1}
h1/c1	1.79	916.50
h1/c3	11.80	497.71
h2/c1	1.24	1008.22
h2/c3	8.17	589.42
h3/c3	3.73	741.92
hh/c3	0.10	1542.67

Table 2. Line pairs (ratios) used to determine the nonuniformity parameter U.
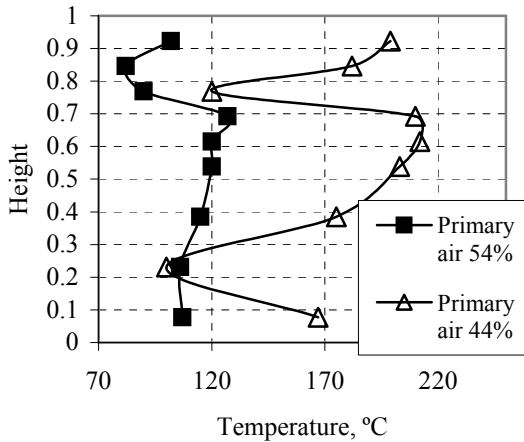
Figure 9. Temperature profile resulting from different air flow-rate ratios to the premixer and secondary air injector.
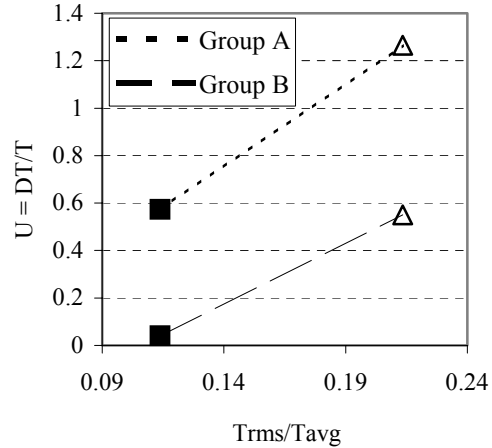
Figure 10. Nonuniformity parameter U_A (open symbols) and U_B (filled symbols) for relatively uniform flow (squares) and less uniform (triangles).

bottom), the combustion products expand downward and mix with the cold stream, resulting in a nearly uniform temperature profile (T_{avg} = 109 ºC, T_{rms} = 12 ºC). It should be noted that there is significant heat loss to the uninsulated combustor walls. This has a large influence on the overall temperature profile. In the second case (44% primary air), the flame gases are hotter (the flame burns closer to stoichiometric), results in a more stratified flow. The high temperature point near the bottom is possibly due to radiative heating of the bottom wall. This profile has T_{avg}=152 ºC and T_{rms}=36 ºC. The sensor output was computed for two different line-pair groups (i.e., two ways to measure U). U_A is based on temperatures interpolated from line ratios h_1/c_1 and h_1/c_3, while U_B is based on h_2/c_1 and h_2/c_3 (Tables 1 and 2). These results are shown in Fig. 10 plotted versus T_{rms}/T_{avg} from the thermocouple readings. The measurements show a significant increase in U_A and U_B with the increase in the temperature nonuniformity of the flow.

B. Synthetic jet mixing control

In these experiments, all flow rates remained fixed (8 scfh methane, 60 scfh premixer air, and 80 scfh secondary air). Mixing control was implemented using the synthetic jet. Results were obtained with no actuation (0 Hz) and for two jet frequencies (40 and 60 Hz). Nominally, this approach should only change the mixing of the hot and cold streams. As seen in the thermocouple temperature profiles (Fig. 11), the synthetic jet array also causes a change in average temperature, due to the enhanced heat loss to the combustor walls with the increase in mixing. Note that the average temperature for these cases (>200 °C) is higher than for air injection control, since the total air flow rate is lower.

As the frequency of the synthetic jet changes from 0 to 60 Hz, mixing increases and we can observe the nonuniformity variable U decreasing in value (Fig. 12). The synthetic jets tend to have a larger influence towards the bottom of the combustor, since they are located there. Two effects are noticeable: the hot region gets wider with the largest effect near the bottom wall, while the peak temperature is driven down. For this case, three nonuniformity
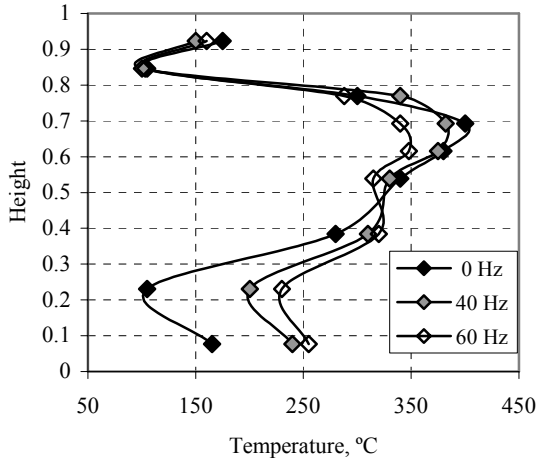
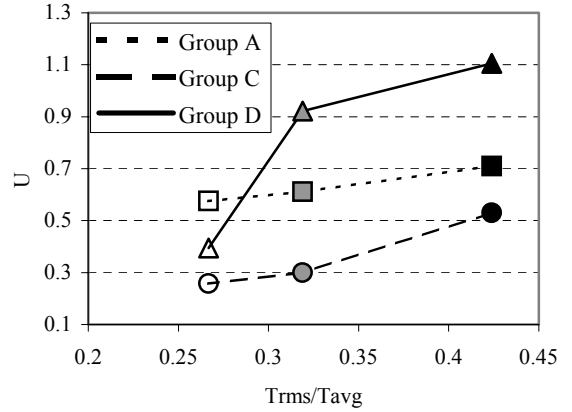**Figure 11. Temperature profile resulting from running the synthetic jet at different frequencies.**

Figure 12. Nonuniformity parameters U for conditions corresponding to running the synthetic jet at 0 Hz (open symbols), 40 Hz (grey symbols), and 60 Hz (black symbols).

variables were computed: U_A is based on line pairs h1/c1 and
h1/c3 (also used in the air injection control results), U_C based on pairs h1/c3 and h3/c3, and U_D (pairs h3/c3 and hh/c3).

While U appears to track T_{rms}/T_{avg} in both control cases, the correspondence of U to T_{rms}/T_{avg} is not unique. This can be seen by comparing the results for a fixed group of line pairs (i.e., U_A) for air injection control and synthetic jet mixing control (Figs. 10 and 12). For example at T_{rms}/T_{avg} of ~0.2, U_A = 1.2 for air injection control, while U_A =0.5 for the synthetic jet mixing. It is possible that U also depends on T_{avg}, since the two flows cases have very different average temperatures. There could also be an influence due to the different water concentration profiles for the two control cases. Further investigations are needed.

VI.   Conclusions

We have demonstrated, experimentally, a pattern factor sensor that is able to track changes in the temperature nonuniformity in the exhaust of a (temperature) stratified combustor. The temperature uniformity is sensed by determining two "weighted" line-of-sight averaged temperatures from ratios of different absorption line peaks. The selection of appropriate line pairs is very important to sensor performance. Line pairs have to be selected for good temperature sensitivity (high lower state energy $\Delta E''$). Individual lines have to be selected with different temperature scaling (both low and high E'' lines) and with similar reference line strengths to limit sensor dynamic range requirements. A uniformity parameter based on the different temperatures was shown to track the changes in the temperature profile (and T_{rms}/T_{avg}) of the combustor exhaust in two separate experiments: when using air injection control and when using synthetic jet mixing control.

This diode laser absorption technique has the following advantages. It is nonintrusive and the sensor can be located remotely with the use of fiber-optics. Because the method employs ratios of absorption lines, it is not strongly sensitive to changes in gas composition. The use of line-peak ratios, rather than spectrally integrated absorption ratios simplifies the hardware and computational requirements and therefore improves the time response of the sensor. In addition, high pressure combustors would probably require the peak ratio approach due to the large amount of line broadening. In the current implementation, water was chosen, since it is a strong absorber and abundant in turbine-engine combustors. While water is a good choice for turbine engine combustor applications, the approach is applicable to other absorbing molecules. Similarly, the use of the 2 μm water bands in the current experiments was dictated by hardware availability.

One major issue affecting sensor performance that remains to be addressed is the importance of other gas properties that can vary along the line of sight. Of primary concern is the composition profile. As illustrated by Eq. (8), the absorber mole fraction profile along the light of sight also affects the "average" temperature from a given line pair and thus can affect U. In a combustor, one would expect the temperature and water mole fraction to be somewhat correlated since higher temperatures would normally correspond to more stoichiometric fuel/air ratios.

However, heat losses to walls can change this relationship. Similarly, composition changes can affect the collision broadening variation across the line of sight and therefore U.

Nevertheless, the current results that show U increasing with the T_{rms}/T_{avg} of the flow, irrespective of how the temperature profile was created, show the promise of this sensor method for pattern factor control. Such a control system would use U as a feedback parameter and actuators, that either control inflow distribution of fuel and air, or downstream mixing actuators like synthetic jets, to drive U down and create a more uniform temperature profile. Future work will investigate the effect of composition profile and methods to incorporate more than two temperatures into a more robust uniformity parameter.

VII.   Acknowledgments

References

[1] Teichert, H., Fernholz, T., and Ebert V., "Simultaneous in situ measurement of CO, H2O, and gas temperatures in a full-sized coal-fired power plant by near-infrared diode lasers," *Applied Optics*, Vol. 42, No. 1220, April 2003, pp. 2043-2051.

[2] Allen, M.G., "REVIEW ARTICLE: Diode laser absorption sensors for gas-dynamic and combustion flows," *Measurement Science and Technology*, Vol. 9, 1998, pp. 545–562.

[3] Zhou, X., Liu, X., Jeffries, J.B., and Hanson R.K., "Development of a sensor for temperature and water concentration in combustion gases using a single tunable diode laser," *Measurement Science and Technology*, Vol. 14, 2003, pp. 1459–1468.

[4] Mihalcea, R.M., Baer, D.S., Hanson, R.K., "Diode-laser absorption measurements of CO_2 near 2 μm at elevated temperatures," Applied Optics, Vol. 37, No. 36, 20 December 1998, pp. 8341-8347.

[5] Rothmana, L.S., Barbeb, A., Chris Bennerc, D., Brownd, L.R., Camy-Peyrete, C., Carleerf, M.R., Chancea, K., Clerbauxf, C., Danae, V., Devic, V.M., Fayth, A., Flaudi, J.M., Gamachej, R.R., Goldmank, A., Jacquemarta, D., Jucksa, K.W., Laffertyl, W.J., Mandine, J.-Y., Massiem, S.T., Nemtchinovn, V., Newnhamo, D.A., Perrini, A., Rinslandp, C.P., Schroederq, J., Smitho, K.M., Smithp, M.A.H., Tangq, K., Tothd, R.A., Vander Auweraf, J., Varanasin, P., Yoshinoa, K., "The HITRAN molecular spectroscopic database: edition of 2000 including updates through 2001," *Journal of Quantitative Spectroscopy & Radiative Transfer*, Vol. 82, 2003, pp. 5–44.

[6] Seitzman, J.M. and Scully, B.T., "Broadband infrared absorption sensor for high-pressure combustion control," *Journal of Propulsion and Power*, Vol. 16, No. 6, pp. 994-1001, 2000.

[7] Seitzman, J.M., Tamma, R., and Scully, B., "Broadband infrared sensor for active control of high pressure combustors," AIAA Paper 98-0401, *Aerospace Sciences Meeting & Exhibit*, 36th, Reno, NV, Jan. 12-15, 1998.

[8] Sanders, S.T., Wang, J., Jeffries, J.B., and Hanson, R.K., "Diode-laser absorption sensor for line-of-sight gas temperature distributions," *Applied Optics*, Vol. 40, No. 24, 20 August 2001, pp. 4404-4415.

[9] Nagali, V. and Hanson, R.K., "Design of a diode-laser sensor to monitor water vapor in high-pressure combustion gases," *Applied Optics*, Vol. 36, No. 36, 20 December 1997, pp. 9518-9527.

[10] Chen, Y, Liang, S, Aung, K, Glezer, A, Jagoda, J, "Enhanced mixing in a simulated combustor using synthetic jet actuators," AIAA Paper 99-0449, *Aerospace Sciences Meeting and Exhibit*, 37th, Reno, NV, Jan. 11-14, 1999.

[11] Chen, Y, Scarborough, D, Liang, S, Aung, K, Jagoda, J, "Manipulating pattern factor using synthetic jet actuators," AIAA Paper 2000-1023, *Aerospace Sciences Meeting and Exhibit*, 38th, Reno, NV, Jan. 10-13, 2000.